Author(s): Hossain, Akbar; Tarvainen, Olli; Reponen, Mikael; Kronholm, Risto; Julin, Jaakko; Kalvas, Taneli; Toivanen, Ville; Kivekäs, Mikko; Laitinen, Mikko

Title: Photo-enhanced O−, H− and Br− ion production in caesium sputter negative ion source : no evidence for resonant ion pair production

Year: 2022

Version: Accepted version (Final draft)

Hossain, A., Tarvainen, O., Reponen, M., Kronholm, R., Julin, J., Kalvas, T., Toivanen, V., Kivekäs, M., & Laitinen, M. (2022). Photo-enhanced O−, H− and Br− ion production in caesium sputter negative ion source : no evidence for resonant ion pair production. Journal of Physics D: Applied Physics, 55(44), Article 445202. https://doi.org/10.1088/1361-6463/ac8e79

Photo-enhanced O^-, H^- and Br^- ion production in caesium sputter negative ion source - no evidence for resonant ion pair production

A. Hossain[1], O. Tarvainen[2], M. Reponen[1], R. Kronholm[1], J. Julin[1], T. Kalvas[1], V. Toivanen[1], M. Kivekäs[1] and M. Laitinen[1]

[1]Accelerator Laboratory, Department of Physics, University of Jyväskylä, FI-40014 Jyväskylä, Finland
[2]STFC ISIS Pulsed Spallation Neutron and Muon Facility, Rutherford Appleton Laboratory, Harwell, OX11 0QX, UK

E-mail: akbar.a.hossain@jyu.fi

August 2022

Abstract. It has been proposed that the negative ion yield of a caesium sputter ion source could be enhanced by promoting neutral caesium atoms to electronically excited 7p states supporting resonant ion pair production. We have tested this hypothesis by illuminating the cathode of a caesium sputter ion source with an adjustable wavelength laser and measuring its effect on the extracted beam currents of O^-, H^- and Br^- anions. The laser exposure causes the beam currents to increase but the effect is independent of the wavelength in the range of 440-460 nm, which leads us to conclude that there is no evidence for resonant ion pair production. The photon-induced beam current enhancement scales with the applied laser power and, depending on the ion source conditions, can more than double the extracted beam current. We present a qualitative explanation for the observed effect. The model, based on photoelectron emission and subsequent increase of the caesium sputtering rate, thus liberating negative ions from the cathode, is supported by the data demonstrating that the caesium sputter ion source can produce Br^- beams without thermal surface ionization as a source of Cs^+ ions, i.e. in external laser-driven mode without heating the surface ionizer.

Keywords: Negative ion source, surface ionisation, caesium sputtering, laser, photoelectric effect

Photo-enhanced O, H and Br ion production in caesium sputter negative ion source - no evidence for resonant ion pair production A. Hossain1, O. Tarvainen2, M. Reponen1, R. Kronholm1, J. Julin1, T. Kalvas1, V. Toivanen1, M. Kivek as1 and M. Laitinen1 1Accelerator Laboratory, Department of Physics, University of Jyv askyl a, FI-40014 Jyv askyl a, Finland 2STFC ISIS Pulsed Spallation Neutron and Muon Facility, Rutherford Appleton Laboratory, Harwell, OX11 0QX, UK E-mail: akbar.a.hossain@jyu.fi August 2022 Abstract. It has been proposed that the negative ion yield of a caesium sputter ion source could be enhanced by promoting neutral caesium atoms to electronically excited 7p states supporting resonant ion pair production. We have tested this hypothesis by illuminating the cathode of a caesium sputter ion source with an adjustable wavelength laser and measuring its effect on the extracted beam currents of O, H and Br anions. The laser exposure causes the beam currents to increase but the effect is independent of the wavelength in the range of 440-460 nm, which leads us to conclude that there is no evidence for resonant ion pair production. The photon-induced beam current enhancement scales with the applied laser power and, depending on the ion source conditions, can more than double the extracted beam current. We present a qualitative explanation for the observed effect. The model, based on photoelectron emission and subsequent increase of the caesium sputtering rate, thus liberating negative ions from the cathode, is supported by the data demonstrating that the caesium sputter ion source can produce Br beams without thermal surface ionization as a source of Cs+ ions, i.e. in external laser-driven mode without heating the surface ionizer. Keywords: Negative ion source, surface ionisation, caesium sputtering, laser, photoelectric effect Photo-assisted negative ion production 2 1. Introduction The negative ion formation in the Source of Negative Ions by caesium Sputtering (SNICS) [1] occurs on the surface of a cathode or "target" containing the ionized material, exposed to caesium ion (Cs+) bombardment [2]. Vogel recently introduced a hypothesis that the negative ion current can be enhanced by exposing the cathode to a laser beam resonantly exciting neutral caesium atoms to 7p electronic states, which acts as a catalyst for negative ion production via so-called ion pair production [3]. It was recently reported [4] that the photo-assisted production of negative ions can be provoked by any laser with the photon energy exceeding a certain threshold, which questioned the resonant ion pair production hypothesis. Further to that, the laser-assisted production of negative ions was observed equally for oxygen with the neutral Cs excited states in resonance with the effective ionization potential of O as well as for aluminium, i.e. Al, in which case the resonant electronic states of Cs were inaccessible with the lasers used at that time [5]. All previous experiments [4, 5] probing the laser- assisted negative ion production in the SNICS have been conducted with off-resonance diode lasers with a very small (if not negligible) fraction of their output power potentially contributing to excitation of the 7p electronic states of Cs from the ground state. Thus, it can be argued that while the previous experiments have revealed a laser-enhancement of the extracted beam current, they have not excluded the possibility of resonant ion pair production contributing to the observed effect. In this paper we report results of laser- assisted negative ion production utilising an adjustable wavelength laser. Tuning the laser wavelength allows exposing the Cs atoms at the SNICS cathode to a flux of photons resonantly exciting the 7p electronic states of Cs, putatively contributing to the ion pair production either directly (H) or via de-excitation to metastable 5d states (O). The beam current enhancement achieved with the tunable laser at the resonant wavelength is compared to results obtained at off-resonance wavelengths. In the Discussion Section we propose an alterna- tive (to ion pair-production) mechanism that could ex- plain the laser-enhancement of the negative ion cur- rent. The discussion is supported by additional results obtained with bromine (Br) ion beam. 2. Experimental setup and procedure The experiment was carried out at the University of Jyv askyl a Accelerator Laboratory (JYFL) with a Multi-Cathode Source of Negative Ions by caesium Sputtering (MC-SNICS) by National Electrostatics Corporation (NEC). The experimental setup is similar to that presented elsewhere [4, 5] with the exception of the laser arrangement. In the following subsections we describe the experimental setup and present the physics arguments for the experimental procedure. 2.1. MC-SNICS ion source The Multi-Cathode Source of Negative Ions by Cae- sium Sputtering (MC-SNICS) [6] produces negative ion beams from a variety of elements by subjecting the ma- terial sample to sputtering by caesium ion bombard- ment [7]. The operation principle of the ion source is described thoroughly elsewhere [1, 4]. Thus, we will describe only the main features of the ion source, rele- vant for

the interpretation of the experimental results presented in this paper. Caesium is evaporated from an external oven into the ion source volume where it con- denses on the surface of the cathode housing the tar- get, hence lowering its effective work function, which enhances the yield of negative ions [8, 9]. Some of the Cs vapor is first adsorbed on the hot surface of the conical tantalum ionizer and then desorbed after a short residence time. The ionizer is brought to sev- eral hundred °C temperature, which according to Saha- Langmuir law, results in large fraction of the desorbed caesium being emitted as Cs+ ions [10]. The Cs+ ions are accelerated towards the target by biasing the cath- ode to kV-range negative potential. The Cs+ ion sput- tering releases particles from the cathode. Some of these particles are ejected as negative ions with the ionisation yield depending on the material (through sputtering rate and electron affinity) and caesium con- centration of the surface affecting the work function of the surface. The surface produced negative ions are accelerated from the cathode by the negative voltage forming the extracted ion beam. The ion beam cur- rent is adjusted by optimising the Cs oven tempera- ture, ionizer temperature, cathode bias and focusing (a.k.a. immersion) lens voltage. The operational prin- ciple of the SNICS ion source is illustrated in Fig. 1.

1. Introduction

The negative ion formation in the Source of Negative Ions by caesium Sputtering (SNICS) [1] occurs on the surface of a cathode or "target" containing the ionized material, exposed to caesium ion (Cs^+) bombardment [2]. Vogel recently introduced a hypothesis that the negative ion current can be enhanced by exposing the cathode to a laser beam resonantly exciting neutral caesium atoms to 7p electronic states, which acts as a catalyst for negative ion production via so-called ion pair production [3]. It was recently reported [4] that the photo-assisted production of negative ions can be provoked by any laser with the photon energy exceeding a certain threshold, which questioned the resonant ion pair production hypothesis. Further to that, the laser-assisted production of negative ions was observed equally for oxygen with the neutral Cs excited states in resonance with the effective ionization potential of O^- as well as for aluminium, i.e. Al^-, in which case the resonant electronic states of Cs were inaccessible with the lasers used at that time [5].

All previous experiments [4, 5] probing the laser-assisted negative ion production in the SNICS have been conducted with off-resonance diode lasers with a very small (if not negligible) fraction of their output power potentially contributing to excitation of the 7p electronic states of Cs from the ground state. Thus, it can be argued that while the previous experiments have revealed a laser-enhancement of the extracted beam current, they have not excluded the possibility of resonant ion pair production contributing to the observed effect. In this paper we report results of laser-assisted negative ion production utilising an adjustable wavelength laser. Tuning the laser wavelength allows exposing the Cs atoms at the SNICS cathode to a flux of photons resonantly exciting the 7p electronic states of Cs, putatively contributing to the ion pair production either directly (H^-) or via de-excitation to metastable 5d states (O^-). The beam current enhancement achieved with the tunable laser at the resonant wavelength is compared to results obtained at off-resonance wavelengths.

In the Discussion Section we propose an alternative (to ion pair-production) mechanism that could explain the laser-enhancement of the negative ion current. The discussion is supported by additional results obtained with bromine (Br^-) ion beam.

2. Experimental setup and procedure

The experiment was carried out at the University of Jyväskylä Accelerator Laboratory (JYFL) with a Multi-Cathode Source of Negative Ions by caesium Sputtering (MC-SNICS) by National Electrostatics Corporation (NEC). The experimental setup is similar to that presented elsewhere [4, 5] with the exception of the laser arrangement. In the following subsections we describe the experimental setup and present the physics arguments for the experimental procedure.

2.1. MC-SNICS ion source

The Multi-Cathode Source of Negative Ions by Caesium Sputtering (MC-SNICS) [6] produces negative ion beams from a variety of elements by subjecting the material sample to sputtering by caesium ion bombardment [7]. The operation principle of the ion source is described thoroughly elsewhere [1, 4]. Thus, we will describe only the main features of the ion source, relevant for the interpretation of the experimental results presented in this paper. Caesium is evaporated from an external oven into the ion source volume where it condenses on the surface of the cathode housing the target, hence lowering its effective work function, which enhances the yield of negative ions [8, 9]. Some of the Cs vapor is first adsorbed on the hot surface of the conical tantalum ionizer and then desorbed after a short residence time. The ionizer is brought to several hundred °C temperature, which according to Saha-Langmuir law, results in large fraction of the desorbed caesium being emitted as Cs^+ ions [10]. The Cs^+ ions are accelerated towards the target by biasing the cathode to kV-range negative potential. The Cs^+ ion sput-

tering releases particles from the cathode. Some of these particles are ejected as negative ions with the ionisation yield depending on the material (through sputtering rate and electron affinity) and caesium concentration of the surface affecting the work function of the surface. The surface produced negative ions are accelerated from the cathode by the negative voltage forming the extracted ion beam. The ion beam current is adjusted by optimising the Cs oven temperature, ionizer temperature, cathode bias and focusing (a.k.a. immersion) lens voltage. The operational principle of the SNICS ion source is illustrated in Fig. 1.

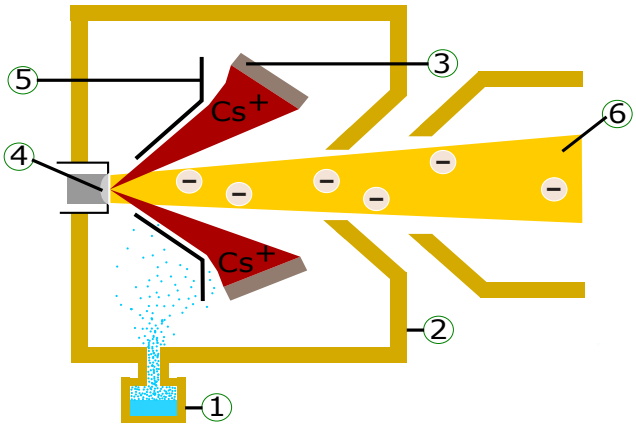

Figure 1. Schematic drawing of the SNICS ion source. (1) caesium oven and transfer line, (2) ionisation chamber, (3) ionizer, (4) cathode, (5) focusing electrode (immersion lens) and (6) extraction channel and electrodes. The relevant dimensions are: 1 mm cathode target diameter, 3 mm cathode holder sleeve diameter, 4.8 mm distance from the cathode to the focusing electrode, 9.8 mm focusing electrode aperture diameter, 21 mm distance from the cathode to the 2.5 mm thick / 6.5 mm diameter ionizer "channel".

2.2. Beamline and beam current measurement

The negative ion beams were extracted from the MC-SNICS source at 12 kV potential, with 4 kV applied to the target and additional 8 kV to the gap lens. The extracted beam was focused with an Einzel lens into a 30° bending magnet for mass-analysis. The beam current transported through the magnet was measured with a Faraday cup. The beam current varied from a few pA to several µA depending on the ionised material and the ion source settings. Thus, a low noise current pre-amplifier (Stanford Research SR570) was used to amplify the Faraday cup signal. The data was visualised and recorded using a Digilent Analog Discovery 2 USB oscilloscope connected to the pre-amplifier. The RC time constant of the measurement setup is 60 µs, which limits the fastest possible pulsing frequency to acquire data. In our experiments the lasers were pulsed and data recorded with up to 10 kHz pulse repetition rates, which are not affected by this time constant. Figure 2 shows a photograph of the low energy beamline with the relevant components identified.

2.3. Laser setup

Two lasers were used in our experiment to enhance the negative ion beam currents. A single-mode diode laser (Toptica DLC DL pro HP) with an adjustable wavelength in the range from 450 nm to 461 nm and an output power up to 160 mW was used to explore the possible contribution of resonant ion pair production on the negative ion yield. The nominal linewidth of the adjustable laser, provided by the manufacturer, is 150–500 kHz, which translates to less than 0.4 fm across the tuning range. Another high power 6 W diode laser (LE-445-6000) with a nominal wavelength of 445 nm was used to study the effect of the laser at elevated beam currents. The full-width-half-maximum (FWHM) linewidth of the high power laser was determined to be 2.7 nm, recorded with Ocean Optics USB 2000+ spectrometer (1.4 nm resolution).

The laser beam illuminates the ion source cathode through a viewport of the 30° dipole magnet (see Fig. 2). Our arrangement differs from the pioneering experiments by Vogel [3] where the laser beam was directed to the volume in front of the cathode through a radial port. In our setup the distance between the laser viewport and the cathode is 1446 mm. To align and focus the laser beam to the cathode through the viewport and ion source extraction aperture we used lenses, mirrors, telescopes and irises as shown in Figure 3. The same optical setup was used for both lasers, except the mirror 8 as it needs to be in place when the high power 445 nm laser is operating and removed from the laser wavelength monitoring path when the Toptica DLC DL pro HP laser is in use. As such, the setup is a compromise between functionality (operation with two lasers) and efficiency as the optics cannot be optimised simultaneously for two different lasers with different focal lengths, output divergences and beam spot sizes.

The Toptica DLC DL pro HP laser was controlled with a Toptica DLC pro digital laser controller. The wavelength was adjusted by a manual (coarse) and piezo-voltage (precision) control of the grating angle. In addition, the laser temperature was controlled to avoid mode hopping in the wavelength range near the 7p excitation resonances. The laser output power was set by adjusting the current of the controller unit between 50 mA and 188 mA, which was found to be a stable range preventing spontaneous mode hopping. A beam sampler [Thorlabs BSF10-B - Ø1" UVFS Beam Sampler] (96:4) was used for the DLC DL pro HP laser to monitor the precise laser wavelength with a

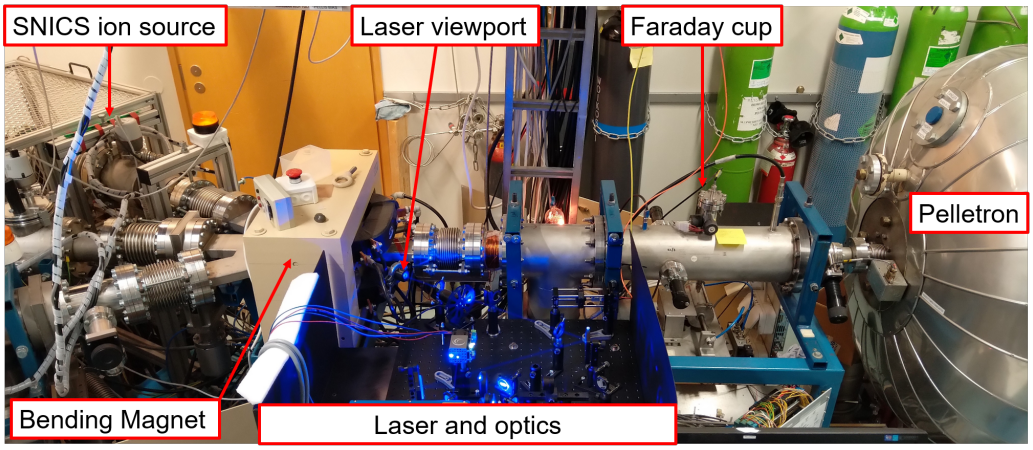

Figure 2. The experimental setup at JYFL accelerator laboratory. The laser beam was focused to the SNICS cathode through the viewport of the bending magnet.

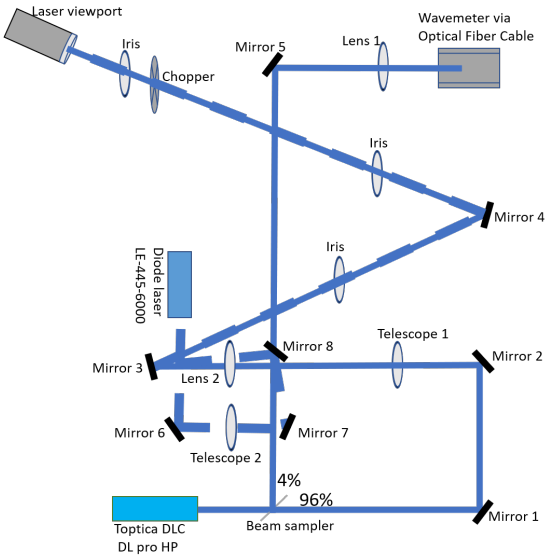

Figure 3. The optical components used for focusing the laser beam onto the ion source cathode via the laser viewport.

HighFinesse Wavelength Meter WS/6-UV, connected to the setup via an optical fibre. The HighFinesse WS/6 unit has been designed for measuring the wavelength of continuous wave and pulse lasers with high accuracy (relative accuracy: 10^{-6} and absolute accuracy: 600 MHz) and measurement rate [11]. A Thorlabs optical chopper (MC2000B-EC) was used to pulse the remaining 96% fraction of the laser beam directed onto the ion source cathode, thus enabling to measure the temporal effect of the laser at varying duty cycles and pulse repetition rates.

The output power, pulse length and pulse repetition rate of the high power LE-445-6000 laser were controlled with a Digilent Analog Discovery 2 - module, which modulates the laser power by supplying an adjustable control voltage and pulse length. The peak wavelength of the high power laser depends on the output power as it affects the temperature and the band gap of the diode. The emission (peak) wavelength in cw mode was recorded with Ocean Optics USB 2000+ spectrometer, which revealed a change from 440 nm to 445 nm when sweeping the output power from 0.3 W to 5.2 W. The peak wavelengths at various output powers within this range can be found from Table S1 in the Supplementary Material. We note that the diode laser wavelength differs significantly from the resonant excitation wavelength (see Fig. 4) of neutral Cs from the ground state to the 7p excited states at all output powers.

2.4. Experimental procedure

The experiment was started by the alignment of the viewport and the SNICS cathode with a telescope. The laser power incident on the cathode surface was then measured by replacing the 1 mm diameter sputter target with a 1 mm diameter collimator (at the cathode location) and a quartz window. The laser power passing through the collimator was measured with a power sensor (Thorlabs S142C integrating sphere photodiode) taking into account the 8% absorption of the quartz window, and compared to the output power of the laser measured in front of the bending magnet viewport. The laser power delivered to the cathode was between 30%-36% of the output power for the adjustable wavelength laser (Toptica DLC DL pro HP) and only 1.2%-3.0% for the LE-445-6000 diode laser after optimising the distances between the optical elements for the adjustable wavelength laser. The efficiency of the diode laser decreases with the output power, i.e. only 1.2% of the photons reached the cathode at the maximum power. The laser power

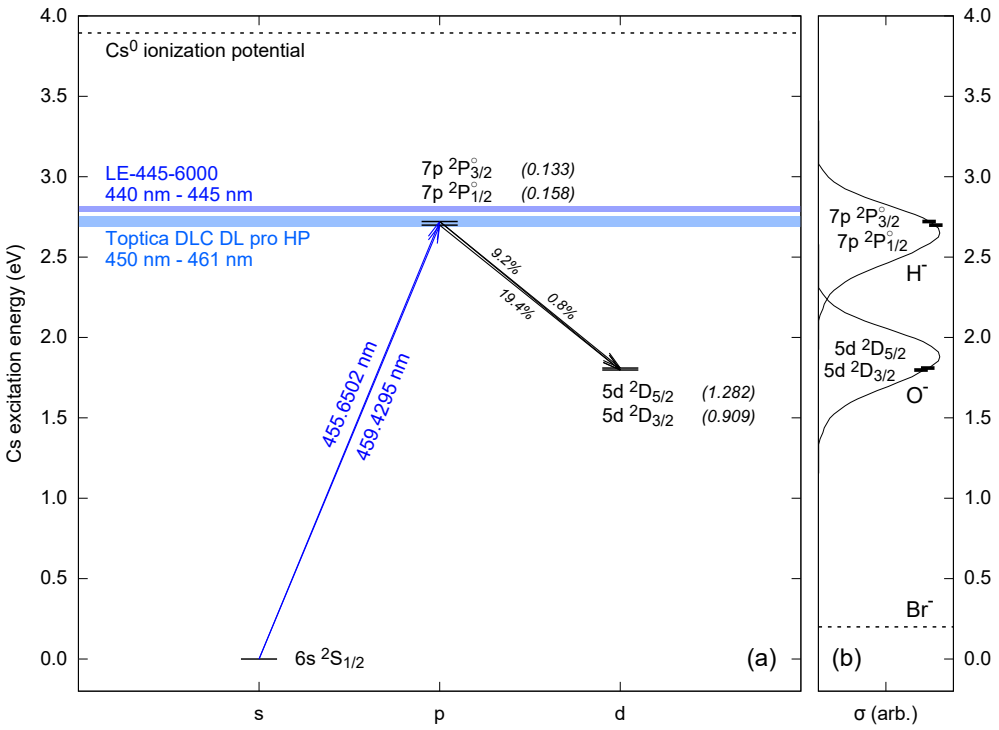

Figure 4. A partial Grotrian diagram of neutral caesium. The diagram (a) shows the putative excitations to 7p-states by the adjustable wavelength laser (Toptica DLC DL pro HP) and the wavelength range of the high power diode laser (LE-445-6000). The marked transitions are accompanied with the corresponding in vacuum wavelengths from Ref. [12]. The radiative decays (in infrared) populating the metastable 5d states that overlap in energy with the normalized O^- ion pair production cross section σ (b) are indicated by black arrows. The pair production cross section of H^- overlaps with the 7p excited states of neutral caesium. The spontaneous lifetime of each excited state in µs is shown in parentheses. The branching ratios of the de-excitations calculated from the reported oscillator strengths[13] are displayed next to each downward transition. The effective ionization potentials of H and O were estimated using electron affinities of 0.754 eV and 1.461 eV, respectively. The effective ionization potential of Br, corresponding to 3.364 eV electron affinity, in hypothetical ion pair production is indicated by a dashed line for completeness.

measured from the cathode and the corresponding efficiency as a function of the output power of each laser are tabulated in Table S2 of the Supplementary Material. The above efficiency numbers are supported by the (off-line) measurement of the laser spot size at the cathode location; the (asymmetric) spot size of the LE-445-6000 diode laser was found to be approximately 4.5 mm by 9 mm whereas the spot size of the Toptica DLC DL pro HP is approximately 2 mm in diameter. It is worth noting that the fraction of the power incident on the 3 mm diameter target holder, which forms part of the cathode assembly is higher. It should be noted that in the earlier experiments, 5%-20% of the diode laser power was measured at the cathode without the 1 mm collimator [5, 4]. Furthermore, the large spot size of the high power laser implies that laser beam is collimated by the extraction channel apertures.

The output power of the adjustable wavelength laser was varied between 34.5 and 56 mW when probing the effect of the laser exposure on the extracted beam currents and pulsing the laser beam with the mechanical chopper. The power was restricted to avoid mode hopping when the wavelength was adjusted "scanning" across the 7p excitation resonances. The whole power range up to 6 W was used for the high power laser (LE-445-6000) to study the extracted beam currents, although the efficiency of the laser power delivered to the cathode degrades at high power due the the mismatch between the laser beam spot size and geometrical apertures. During the experiments we adjusted some of the optical elements when optimising the extracted beam currents and, thus, in the following sections we will use the laser output powers to indicate the experimental conditions.

Three cathode materials were used in this experiment. They were prepared by pressing either Al_2O_3, TiH or CsBr powder into the 1 mm (in diameter) cylindrical notch of the aluminum cathode sleeve. The Cs^+ ions were accelerated towards the cathode by applying a 4 kV negative potential to it and focused into the front face of the cathode by the "focusing (or immersion) lens", located 5 mm from the cathode and biased to 1 kV positive potential. These voltages were kept constant for all measurements. The

beam currents of O^- (from Al_2O_3), H^- (from TiH) and Br^- (from CsBr) were adjusted by controlling the ionizer heating power (surface temperature) and the Cs oven temperature, which affect the flux of Cs^+ ions incident on the cathode and the cathode work function via the neutral Cs deposition rate, respectively. The ion source was allowed to settle for half an hour as a minimum between cathode changes to achieve stable operation.

The adjustable laser (Toptica DLC DL pro HP) was tuned for the resonant wavelengths of the electronic excitation to $7p_{1/2}$ and $7p_{3/2}$ states of neutral Cs, which are allegedly in resonance for the pair production of H^- anions, or decay to the metastable 5d states, which are in resonance for the pair production of O^-. The branching ratio to the 5d states is 10-20% depending on the upper state, whereas the spontaneous lifetime of the 5d states is 6-10 times longer than the lifetime of the 7p states. Thus, it can be expected that the interaction probability of 7p-excited Cs atoms and H^0 neutrals or 5d-excited Cs atoms and O^0 neutrals is on the same order of magnitude, assuming equal neutral densities. The pair production hypothesis is illustrated in Fig. 4 showing a partial Grotrian diagram of neutral Cs and the projected pair production cross sections of O^- and H^-. The ion pair cross sections are based on the electron exchange probability obtained from Landau-Zener-Stückelberg (LZS) formalism [14, 15, 16]. The electron transfer is considered resonant when the effective ionization potential, $I_{p,\mathrm{eff}}$, of the electronically excited donor atom equals the sum the acceptor atom's electron affinity E_A and the reaction endothermicity ΔE i.e. $I_{p,\mathrm{eff}} = E_A + \Delta E$. The effective ionization potential (in eV units) corresponding to the above resonance condition can be estimated from a semi-empirical power fit to experimental data [17], i.e. $I_{p,\mathrm{eff}} = E_A \left(\frac{4.72}{E_A}\right)^{0.275}$, which has been used to calculate the effective ionization potentials of H, O and Br in Fig. 4.

The negative ion beam currents achieved at the resonant wavelengths populating the 7p states of neutral Cs were compared to those achieved with off-resonance wavelengths of the laser. Furthermore, we estimated the maximum Doppler broadening of the absorption line to be approximately 0.66 pm at the resonant wavelengths. The Doppler broadening was calculated from $\Delta\lambda = (\lambda/c)\sqrt{(2kT)/m_{Cs}}$, where λ is the wavelength, c is the velocity of light, m_{Cs} is the mass of caesium atom, the Boltzmann constant $k = 1.38 \times 10^{-23}$ J/K. The given maximum broadening corresponds to Cs temperature of 1500 K, which is the highest conceivable ionizer temperature. The effect of the laser exposure on the negative ion currents was measured at off-resonance wavelengths within and outside the Doppler profile of the absorption lines to account for the possibility of the line broadening affecting the interpretation of the results. The experimental data were taken with O^-, H^- and Br^- using different ionizer powers (temperatures) and laser pulse patterns and powers.

In the last stage of the experiment with Br^-, we recorded the effect of the laser exposure on the cathode current, which was measured from the output of the cathode high voltage power supply. In order to probe the relevant physical mechanisms, the effect of the laser exposure on the Br^- beam current was measured with and without heating the ionizer as well as with and without heating the Cs oven.

3. Experimental results

3.1. Oxygen (O^-)

The measurements were started by demonstrating that the laser-enhancement can be observed at various ion source settings corresponding to an order of magnitude different O^- beam currents. Furthermore, it was confirmed that pulsing the laser with the chopper results in similar response of the beam current as pulsing the laser by modulating the control voltage, which enables us to compare the results obtained with the two lasers. The details of the latter are presented in the Supplementary Material.

Figures 5(a) and 5(b) show examples of the laser enhancement measured at order of magnitude different O^- beam current. The prompt increase of the beam current when the laser pulse is applied is clearly visible in both cases. The given examples are measured with the LE-445-6000 diode laser with 2.3 W output power resulting in 17% increase of the beam current, and with the adjustable wavelength laser with 49 mW power at 455.5241 nm resulting in 4-6% gain. Figures 5(c) and 5(d) show the corresponding Fast Fourier Transform (FFT) spectra, which demonstrate that the beam current modulation follows the 40 Hz and 70 Hz pulsing frequency of the laser beam by the control voltage or mechanical chopper, respectively. The noise peak at 50 Hz is due to the AC line frequency coupling into the experimental setup. It is worth noting that the laser wavelengths used for Figs. 5 are not in resonance with the excitation energies of the 7p states of neutral caesium from the ground state, which casts doubt on the ion pair production hypothesis as already pointed out in Ref. [3].

Thus far, the presented data (including Refs. [4, 5]) do not exclude the possibility of ion pair production contributing to the beam current at the laser wavelength(s) resonant with the excitation of 7p states. In order to establish whether the excitation of these states affects the extracted O^- beam current, the Al_2O_3 cathode was irradiated with the adjustable laser

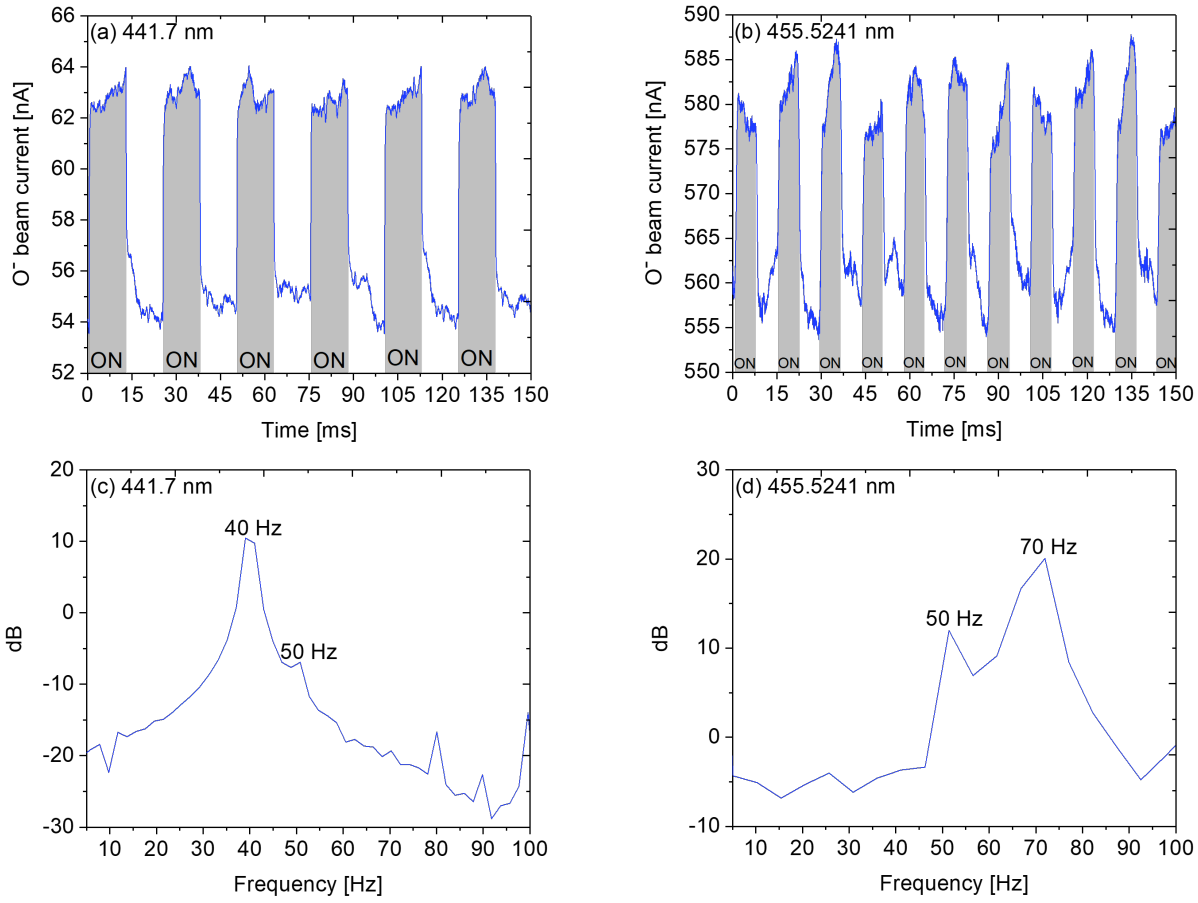

Figure 5. Examples of the prompt laser enhancement at different order of magnitude O^- beam currents: The effect of (a) LE-445-6000 diode laser with 2.3 W output power at 40 Hz repetition rate and (b) the Toptica DLC DL pro HP laser with 49 mW output power at 70 Hz repetition rate. The corresponding Fast Fourier Transform spectrum of the beam current are shown in (c) and (d), respectively.

scanning the wavelength across the excitation photon energies. The chopper frequency was set to 70 Hz and the laser output power varied from 34.5 mW to 49 mW.

Figures 6 and 7 show the response of the O^- beam current with three different laser wavelengths. Figures 6(a) and 7(a) illustrate the wavelength selection with a depicted Doppler-broadened (Gaussian) absorption line. The depicted Doppler broadening corresponds to the highest conceivable ionizer temperature, i.e. in the experiment the line width is most likely more narrow. The wavelengths in sub-figures 6(b) and 7(b) correspond to the (in-vacuum) excitation wavelengths[12] of the $7p_{1/2}$ and $7p_{3/2}$ states of neutral Cs, respectively. The remaining two wavelengths are off-resonance, one of them in 6(c) and 7(c) within the expected Doppler broadening of the absorption lines, and the remaining one in 6(d) and 7(d) outside the expected Doppler profile. In all cases the O^- beam current enhancement is 3-6%. The variation between the wavelengths is attributed to the natural temporal stability of the SNICS ion source, not to the variation of the laser wavelength, whereas the difference between the laser pulses within each data set is related to the 50 Hz noise signal.

It is important to note that although the data presented here corresponds to discrete wavelengths, during the experiment we scanned the adjustable laser across 455.5241 nm - 455.7085 nm and 459.3153 nm - 459.4429 nm ranges blanketing the resonant wavelength for the excitation of 7p states of neutral caesium without observing an increase of the laser enhancement nor a disappearance of the laser effect. Such scan eliminates the possibility of a systematic error in the detection of the wavelength.

The observation leads to two conclusions: (i) resonant ion pair production involving 7p excited neutral caesium does not contribute to the O^- production in this experiment even when the power at the resonant excitation wavelength is increased by several orders of magnitude in comparison to

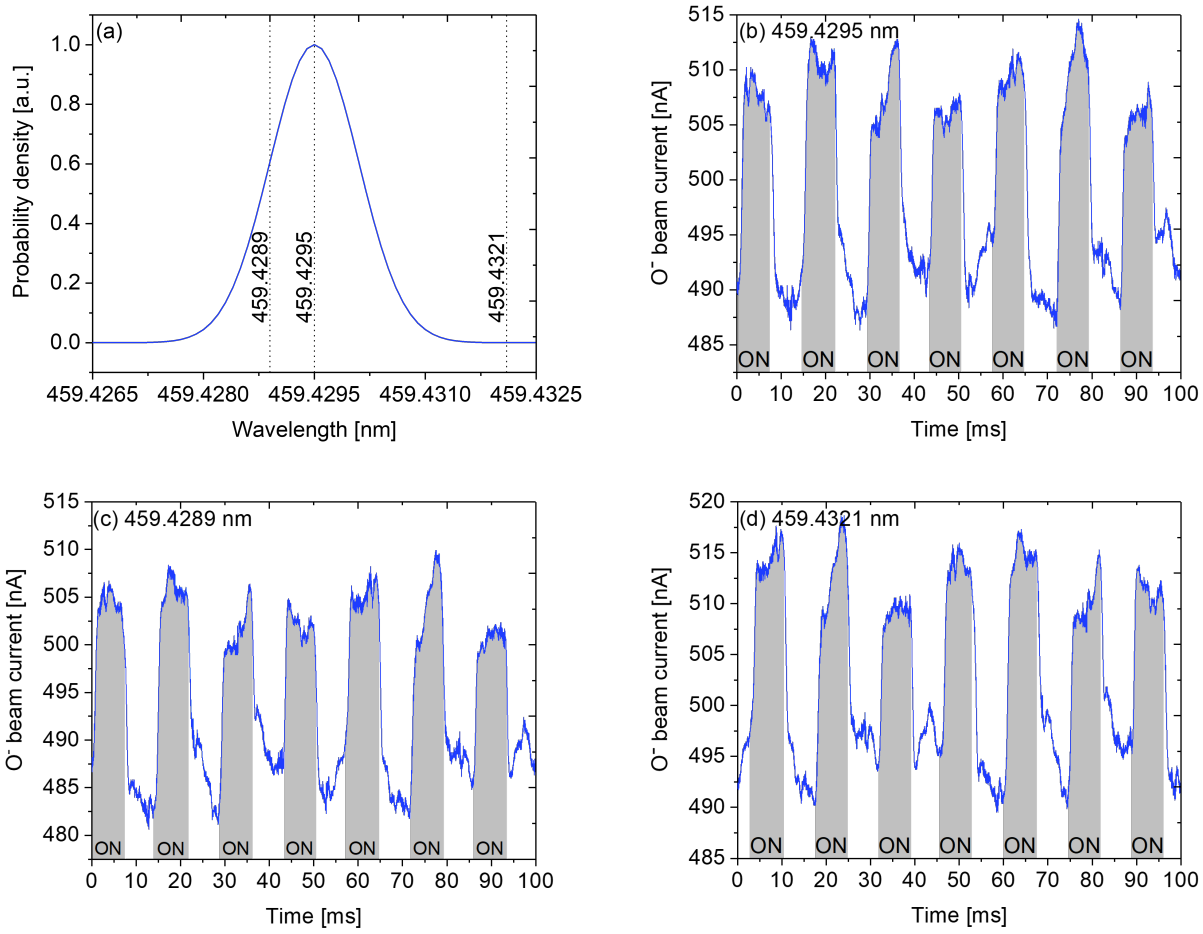

Figure 6. Wavelength selection for the excitation of the $7p_{1/2}$ electronic state of neutral Cs: (a) shows the expected maximum Doppler broadening of the absorption line and the laser wavelengths used for probing the putative ion pair production. The prompt effect of the laser exposure on the O^- beam current with different wavelengths: (b) in-vacuum resonance at 459.4295 nm, (c) 459.4289 nm within the maximum Doppler broadening, and (d) 459.4321 nm outside the maximum Doppler broadening.

earlier experiments [4, 5], and (ii) the experimental setup is suitable for studying the ion pair production hypothesis. The latter follows from the experiments with the adjustable wavelength laser proving that caesium absorption along the laser beam path does not prevent the photon flux from reaching the cathode, which would lead to disappearance of the laser enhancement despite of the physical mechanism in action. In other words, the Cs density in the ion source volume is not prohibitively high for probing the effect.

3.2. Hydrogen (H^-)

The experiments were continued using a TiH-cathode to study the laser-induced effect on the H^- beam current. Figure 8(a) demonstrates the laser enhancement for H^- for the first time. In the given example the beam current increased by approximately 12% with 49 mW laser output power at 455.52 nm. Unlike in the case of oxygen, the laser effect was not instantaneous but instead it took approximately 370 ms to reach the peak of the current. A slow gradual decrease of the beam current is observed after the initial gain. We associate this behaviour to the changing Cs coverage and work function of the cathode. Figure 8(b) shows the effect of the laser power on the H^- beam current. The four steps highlighted with gray background correspond to pulses at 1 W, 2.3 W, 3.6 W and 4.7 W laser output powers. As the laser power was increased, the wavelength varied from 440.7 nm to 443.9 nm. A prompt enhancement as well as a gradual (slow) increase of the beam current is observed when the laser pulse is applied. The H^- beam current is approximately doubled at 4.7 W laser output power, i.e. the current increases from the original level of 800 nA to 1700 nA (113%). It is also notable that the time constant related to the gradual increase of the beam current becomes shorter at high laser power

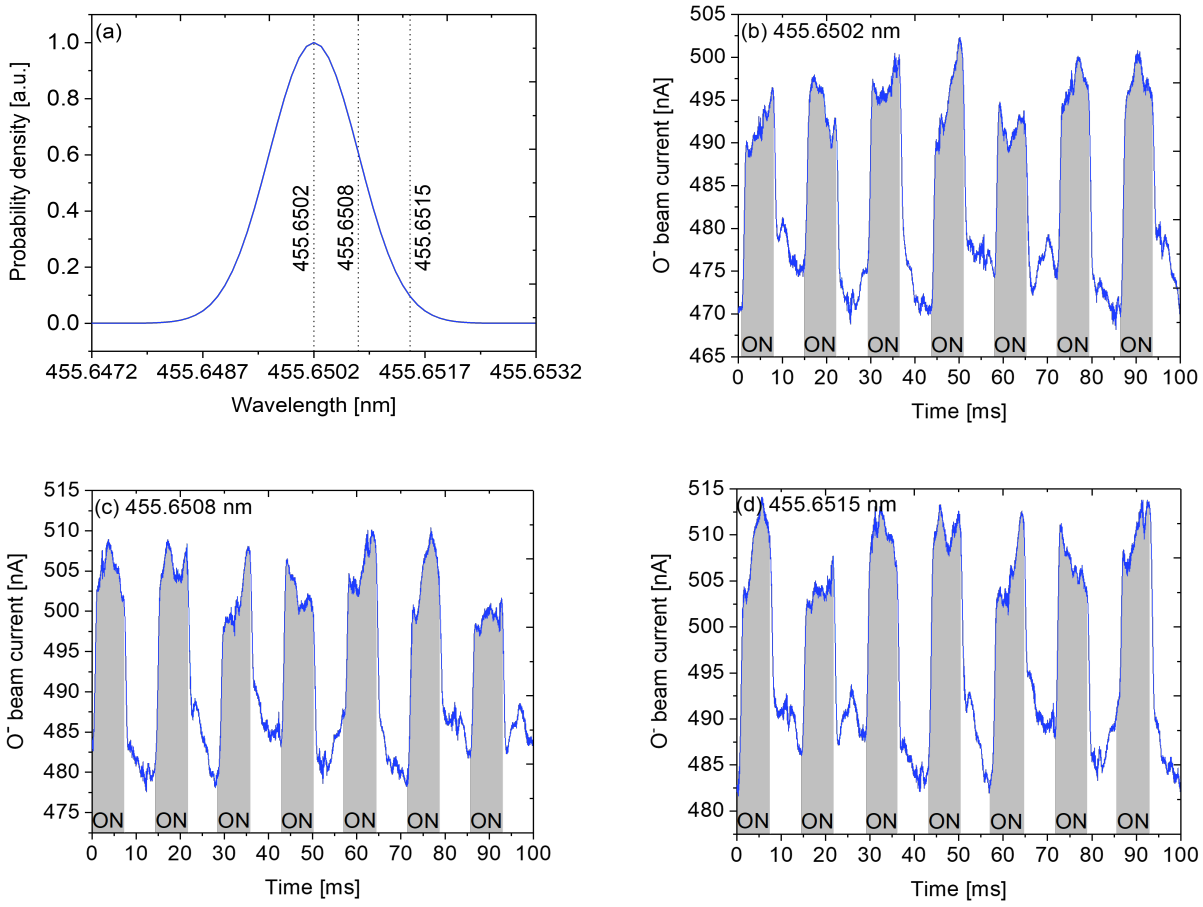

Figure 7. Wavelength selection for the excitation of the $7p_{3/2}$ electronic state of neutral Cs: (a) shows the expected maximum Doppler broadening of the absorption line and the laser wavelengths used for probing the putative ion pair production. The prompt effect of the laser exposure on the O^- beam current with different wavelengths: (b) in-vacuum resonance at 455.6502 nm, (c) 455.6508 nm within the maximum Doppler broadening, and (d) 455.6515 nm outside the maximum Doppler broadening.

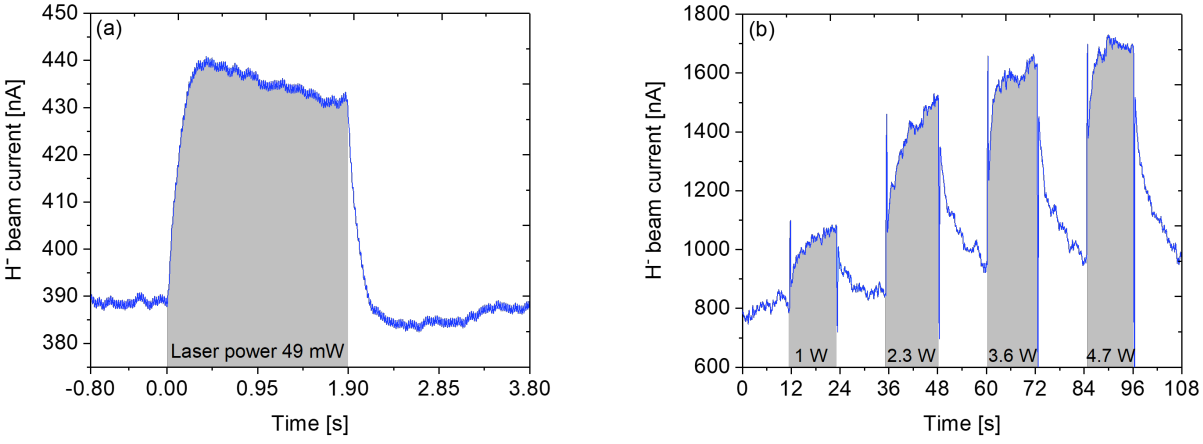

Figure 8. The effect on the H^- beam current for the (a) Toptica DLC DL pro HP laser with 49 mW laser output power at 455.52 nm wavelength and (b) the effect of the LE-445-6000 diode laser output power on the H^- beam current. The laser pulse length is 1.90 s in (a) and 12 s in (b), both having a 50% duty factor.

implying a thermal origin for the slow response as discussed in Ref. [4]. The cathode temperature can be expected to affect the equilibrium Cs density and, subsequently, the work function of the cathode surface, which in turn affects the negative ion yield at certain Cs^+ ion flux. Thus, the laser not only amplifies the negative ion production promptly but it can also be used for "cathode conditioning".

In addition to demonstrating the laser-enhanced H^- production and its power-dependence, we used the adjustable wavelength laser to further probe the ion pair production hypothesis. The TiH cathode was irradiated with wavelengths corresponding to the electronic excitation from the ground state to $7p_{3/2}$ state of neutral Cs, which are allegedly in resonance for the pair production of H^- anions. In this case the chopper frequency was set to 20 Hz and approximately 49 mW laser output power was used when the laser wavelength was swept across the excitation wavelength starting and ending with an off-resonance photon energy. The sweep was carried out at wavelength ranges of 455.6462 nm to 455.6535 nm without observing any difference in the H^- beam current. Thus, we conclude that the laser enhancement of the H^- beam current (from TiH cathode) is not wavelength sensitive. However, its magnitude depends on the laser power, which together imply that the laser amplifies an already existing negative ion production pathway. As such, the result is similar to that obtained with O^- ion beam, i.e. there is no evidence for ion pair production contributing to negative ion formation in the SNICS ion source. In fact, the prompt enhancement of the H^- beam current with 49 mW laser output power was only 0.5-1% (regardless of the wavelength), barely observable above the noise present in the beam current but clearly visible in the Fast Fourier Transform spectrum as shown in Fig. 9. The reason for the prompt laser enhancement being weaker for H^- (than for O^-) but the long-term exposure more than doubling the beam remains elusive, but it is most likely related to "conditioning" of the cathode Cs coverage by the laser.

3.3. Bromine (Br^-)

The results obtained with O^- and H^- beams with putative ion pair production resonances with 5d and 7p states of neutral Cs have lead to the conclusion that ion pair production is very unlikely to contribute to the observed laser enhancement of the negative ion beam currents. This motivated us to probe the laser effect with a Br^- beam, relevant for ion beam analysis, namely Time-of-Flight Elastic Recoil Detection Analysis (TOF-ERDA) at JYFL [18]. It is worth noting that the effective ionisation potential of Br^- (see Fig. 4) is far from the excited state energy levels of neutral Cs, i.e. ion pair-production from the excited states of Cs, described by Vogel [3], cannot contribute to the negative ion yield. On the other hand, as the negative ion yield depends strongly on the work function of the cathode, which is sensitive to the Cs coverage [19, 20], it could be expected that the laser-induced effect is temporally stable with the Cs-containing cathode materials such as CsBr.

Figure 10(a) shows an example of the laser enhancement on Br^- beam current with approximately 3.6 W laser output power at 442.8 nm wavelength (LE-445-6000 laser) at 10 Hz pulse frequency and 60% duty factor. In this case the Br^- beam current gain is approximately 155%, i.e. from 820 nA to 2090 nA. The observed gain implies that either the response of the negative ion beam produced from the Cs compound cathode material is stronger by nature or the electron affinity of the negative ion affects the laser enhancement factor. Figure 10(b) shows the longer term effect of the laser on the Br^- beam current. In this case we applied 4.7 W laser output power at 443.9 nm wavelength with 16.7 mHz pulse frequency and 60% duty factor, i.e. 36 s pulses every 60 s. In this case the beam current increased by approximately 58%, i.e. from 1900 nA to 2995 nA. The data in Figs. 10(a) and 10(b) were recorded under slightly different ion source settings, i.e. ionizer heating powers of 17 A for (a) and 16 A for (b), which affects the beam current and the gain achieved by applying the laser beam. Both data sets indicate a prompt effect on the extracted beam current, while Fig. 10(b) demonstrates that the laser enhancement can be maintained for longer periods.

In addition, we demonstrated the prompt effect of the laser with high pulse repetition rates, up to 10 kHz, which are not relevant for the applications of the SNICS ion source in our setup but could be of interest for pulsed beam applications. Examples of the laser enhancement at 1-10 kHz repetition rates can be found from the Supplementary Material (Figure S2).

Altogether the presented data suggests that the laser enhancement could potentially be observed for all negative ion species produced with the SNICS ion source, not only for those species with their effective ionisation potential aligning with the energy levels of excited states of neutral Cs.

4. Discussion

The experiments described in this paper have developed the understanding of the laser-assisted enhancement of negative ion production in caesium sputter ion sources. The fact that both, O^- and H^- beams exhibit a similar laser-enhancement at resonant and off-resonant laser wavelengths (for the excitation of neu-

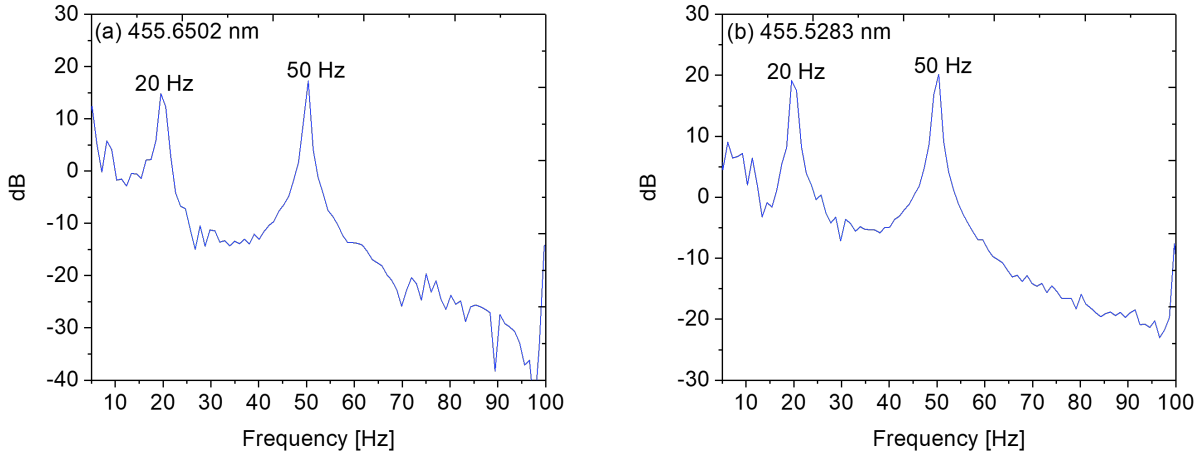

Figure 9. An example of the Fast Fourier Transform (FFT) spectrum of the H^- beam current for 455.6502 nm laser wavelength corresponding to in-vacuum resonant excitation of the $7p_{3/2}$ state of neutral Cs (a) and for 455.5283 nm off-resonance wavelength outside the expected Doppler broadening profile of the excitation resonance (b).

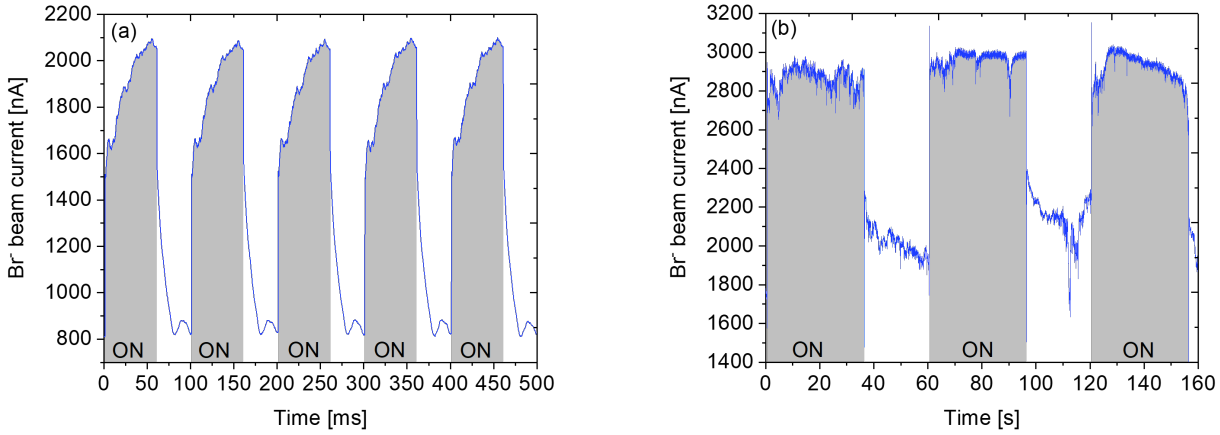

Figure 10. The effect on the Br^- beam current with (a) 3.6 W laser output power at 442.8 nm wavelength and (b) 4.7 W laser output power at 443.9 nm wavelength incident on the cathode. The laser pulse period is (a) 100 ms and (b) 60 s with 60% duty factor.

tral Cs to 7p electronic states), together with the effect being found equally for Br^-, confirms that the observed effect is not due to ion pair production. Conversely, we have not found any evidence for the existence of ion pair production in the SNICS ion source while the laser photons evidently are not absorbed by the Cs vapor but instead reach the cathode also at the resonant wavelength. The experimental evidence leads to the conclusion that the laser amplifies an already existing negative ion production pathway and, thus, the effect most probably exists for all negative ion species. The magnitude of the effect can be expected to depend on the ion source conditions, in particular the caesium vapor pressure, which influences the sputtering rate and the work function of the cathode material.

The present understanding allows us to formulate the following qualitative model for the sequence of events explaining the laser enhancement mechanism, as illustrated in Fig. 11: (i) The laser photons induce photoelectron emission from the low work function cathode. (ii) The emitted electrons are accelerated by the cathode bias ionizing Cs atoms in the ion source volume adjacent to the cathode. (iii) The Cs^+ ions produced via electron impact ionization are drawn towards the cathode along with the surface ionised Cs^+ (from the ionizer), promptly increasing the sputtering rate of the target and its negative ion yield. (iv) In addition, the increased sputtering rate and temperature of the cathode affect the Cs balance and the work function of the surface, which explains

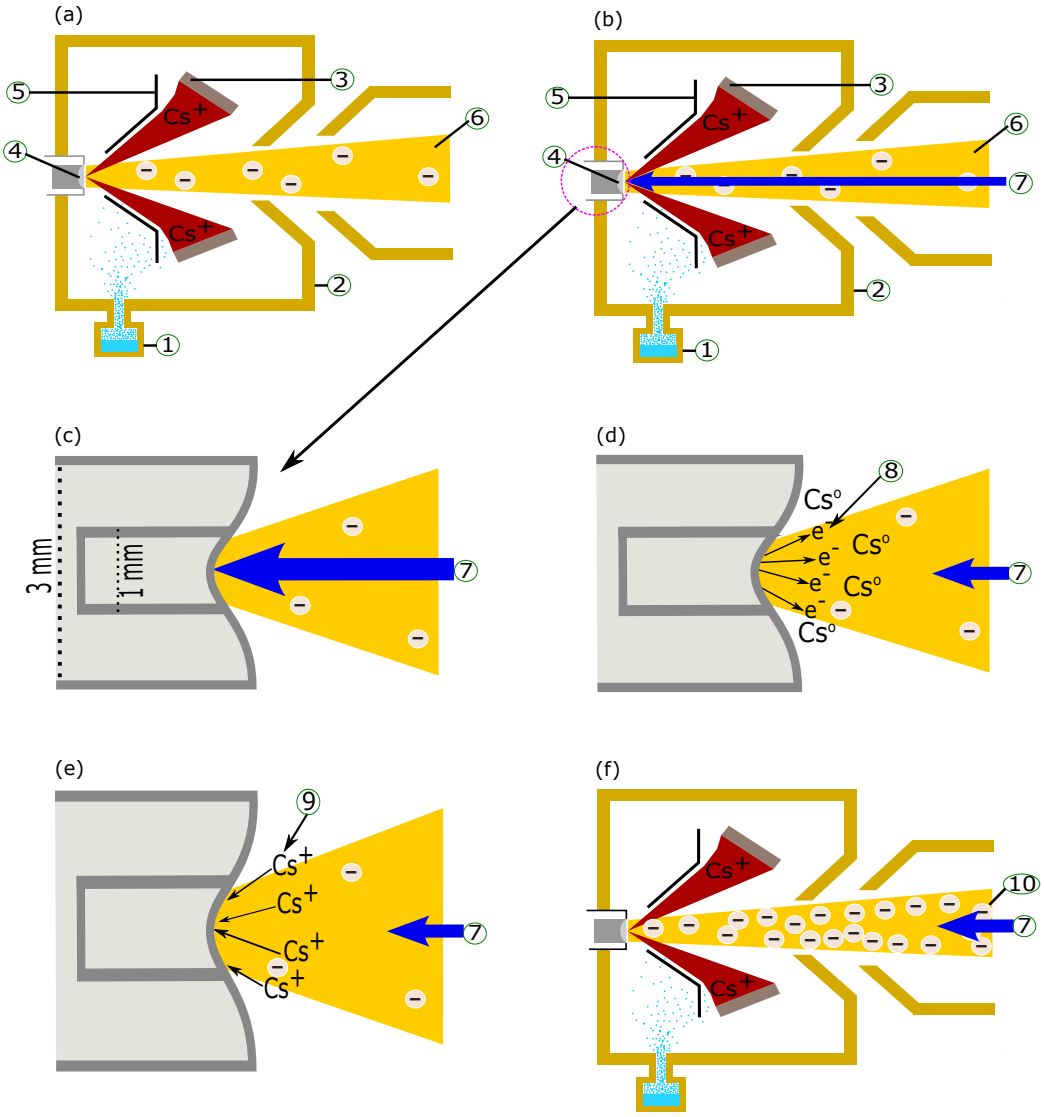

Figure 11. A schematic drawing of the SNICS ion source (a) and the illustration of the proposed photo-assisted negative ion production mechanism (b)-(f). The applied laser beam (c) induces photoelectron emission from the cathode (d) resulting in volumetric ionization of the Cs vapor (e). The enhanced Cs^+ bombardment of the cathode increases the negative ion yield, i.e. the beam current in (f) is higher than the original beam current in (a). The labeling refers to the following: (1) caesium oven and transfer line, (2) ionization chamber, (3) ionizer, (4) cathode, (5) focusing electrode (immersion lens), (6) extraction channel and electrodes, (7) laser beam, (8) emitted photoelectrons, (9) ionised Cs^+ and (10) increased negative ion yield.

the slow variation of the negative ion yield, i.e. either a gain or loss of the beam current, with the time constant of the transient depending on the applied laser power. The proposed mechanism is illustrated in Fig.11. It is worth noting that the increased ion bombardment of the cathode and its holder increases the emission flux of secondary electrons, which in turn results in increased ionisation rate of the Cs vapour, thus amplifying the photon exposure effect. However, the contribution of the ion induced secondary electrons cannot be quantified.

The qualitative model is supported by the fact that the prompt effect on the O^- beam is not observed at laser wavelengths $\geq$520 nm, i.e. at photon energies $<$2.38 eV [4]. Such threshold effect could be explained by the work function of the cathode or the cathode holder surface being higher than 2.38 eV, thus preventing photoelectron emission at energies below the work function threshold. It is emphasized that this threshold, together with the photo-assisted enhancement, would depend strongly on the Cs balance and work function of the cathode or the cathode holder surface, illuminated by the laser.

In order to collect implicit evidence for our model we measured the change of the cathode current from a CsBr target as a function of the applied laser power

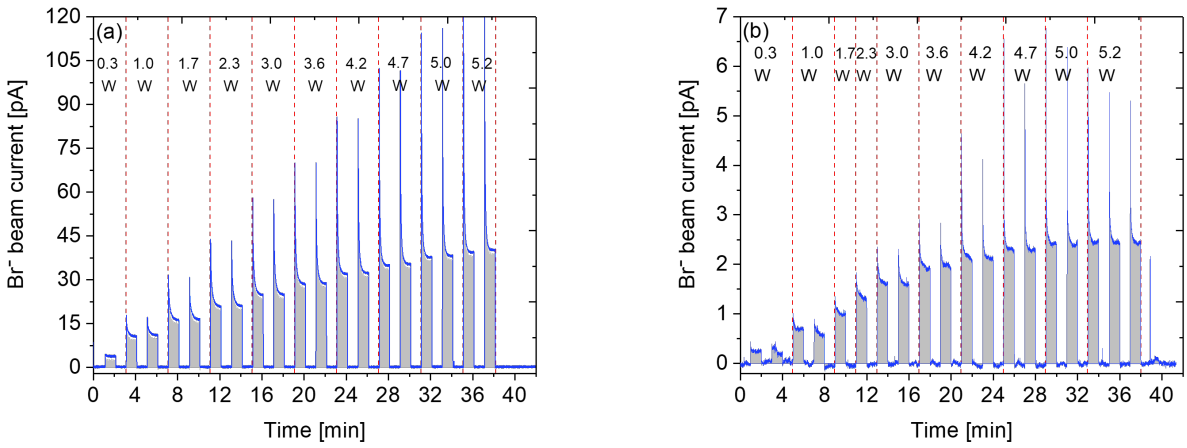

Figure 12. The effect on the Br^- beam current for the 6 W diode laser. The data was measured with 5.5 A ionizer current and (a) 160 °C Cs oven temperature, (b) without the Cs oven ON. The laser pulses are highlighted with gray background and the corresponding laser pulse powers are shown on the top of the Figure.

and compared it to the regular operation of the ion source without the laser at 17 A ionizer current. The (total) cathode current consists of inbound Cs^+ ions, and outbound negative ions and electrons (secondary and photoelectrons). The cathode currents shown in Table 1 were measured with the LE-445-6000 laser. We observed that the cathode current increases instantly when laser is turned ON. The increase of the cathode current scales with the laser output power and efficiency of the power delivered to the cathode (see Table II in the Supplementary Material). At high laser power the cathode current almost doubles, which matches rather well with the change of the negative beam current observed for Br^- (see Fig. 10).

Table 1. The cathode current with the laser OFF and ON with different laser powers at 17 A ionizer current and 160 °C Cs oven temperature. The data were taken with 16.67 mHz pulse frequency and 50% duty factor, i.e. 30 s pulses every 60 s.

Laser Power	Cathode current	Cathode current
Output power [W]	Laser OFF [mA]	Laser ON [mA]
0.3	0.22	0.25
1.0	0.22	0.32
1.7	0.22	0.36
2.3	0.23	0.38
3.0	0.23	0.39
3.6	0.23	0.40
4.2	0.23	0.41
4.7	0.23	0.42
5.0	0.23	0.42
5.2	0.23	0.43

The effect of the laser on the cathode current motivated us to conduct a further experiment at 5.5 A ionizer current and 160 °C Cs oven temperature. In such configuration the flux of surface ionized Cs^+ ions from the ionizer to the cathode is negligible resulting in no negative ions being extracted in normal operation of the SNICS ion source, i.e. without the laser. Table 2 shows the effect of the LE-445-6000 laser power on the cathode current for 5.5 A ionizer current. In this case, the cathode and beam currents are non-zero only when the laser is turned ON, both scaling with the laser power. We also observed up to 40.2 pA Br^- ion beam current when the laser was ON as shown in the Table 2 and corresponding Fig. 12(a) showing the pulsed laser-driven beam. The rising and falling edges of the laser-induced beam current pulses are instantaneous with the laser pulsing. The effect of the laser is persistent for several minutes. The observation supports our qualitative model of photoelectrons ionizing neutral Cs in the ion source volume, which results in Cs^+ bombardment of the cathode inducing negative ion emission.

This observation motivated us to run yet another experiment with Br^- beam at 5.5 A ionizer current and Cs oven turned off. The result is shown in Fig. 12 (b). Comparing the two data sets in Fig. 12 reveals that the vapor pressure of the neutral Cs, which is controlled by the Cs oven temperature, affects the laser-induced Br^- beam current. Again, this is expected as, according to our model of the photo-assisted ionization, the Cs vapor pressure in the ion source volume defines the volumetric ionization rate by photoelectrons.

In conclusion, our results have disputed the hypothesis of laser-induced ion pair production contributing to the negative ion beam currents of the SNICS ion source when the cathode face is illuminated by an external laser. However, the experiments have opened the door for the design of laser-driven ion source requiring only Cs vapor to operate, but not a hot

Table 2. The cathode current with the laser OFF and ON with different laser powers at 5.5 A ionizer current and 160 °C Cs oven temperature. The data were taken with 8.33 mHz pulse frequency and 50% duty factor, i.e. 60 s pulses every 120 s.

Laser Power	Cathode current	Cathode current	Beam current
Output power [W]	Laser ON [mA]	Laser OFF [mA]	[pA]
0.3	0.01	0	4.0
1.0	0.03	0	11.3
1.7	0.04	0	16.8
2.3	0.05	0	21.3
3.0	0.06	0	25.2
3.6	0.06	0	28.7
4.2	0.07	0	32.4
4.7	0.07	0	35.7
5.0	0.07	0	38.2
5.2	0.07	0	40.2

surface (ionizer) for Cs^+ ionization. The beam currents extracted from such ion source could be optimised by improving the laser optics. Further exploration of the laser-cathode interaction is needed to fully optimise the output from such a laser-driven ion source.

Data availability statement

The data that support the findings of this study are available from the corresponding author upon reasonable request.

Acknowledgements

Patent application (number 20225597) has been filed to the Finnish Patent and Registration Office.

REFERENCES

[1] Alton G D 1990 *Tsukuba Polarized Workshop 1990:0339-374, Report number: CONF-900289-4* URL https://digital.library.unt.edu/ark:/67531/metadc1191487/

[2] Williams P 1979 *Surface Science* **90** 588–634 ISSN 0039-6028 URL https://www.sciencedirect.com/science/article/pii/0039602879903637

[3] Vogel J S 2019 *Nuclear Instruments and Methods in Physics Research Section B: Beam Interactions with Materials and Atoms* **438** 89–95 ISSN 0168-583X URL https://www.sciencedirect.com/science/article/pii/S0168583X18304282

[4] Tarvainen O, Kronholm R, Laitinen M, Reponen M, Julin J, Toivanen V, Napari M, Marttinen M, Faircloth D, Koivisto H and Sajavaara T 2020 *Journal of Applied Physics* **128** 094903 URL https://doi.org/10.1063/5.0020751

[5] Tarvainen O, Kronholm R, Laitinen M, Reponen M, Julin J, Toivanen V, Napari M, Marttinen M, Kalvas T, Faircloth D, Koivisto H and Sajavaara T 2021 *AIP Conference Proceedings* **2373** 020001 URL https://aip.scitation.org/doi/abs/10.1063/5.0057495

[6] Middleton R 1983 *Nuclear Instruments and Methods in Physics Research* **214** 139–150 ISSN 0167-5087 URL https://www.sciencedirect.com/science/article/pii/016750878390580X

[7] Krohn V E 1962 *Journal of Applied Physics* **33** 3523–3525 URL https://doi.org/10.1063/1.1702439

[8] Yu M L 1978 *Phys. Rev. Lett.* **40**(9) 574–577 URL https://link.aps.org/doi/10.1103/PhysRevLett.40.574

[9] van Os C F A, Granneman E H A and van Amersfoort P W 1987 *Journal of Applied Physics* **61** 5000–5011 URL https://doi.org/10.1063/1.338320

[10] Taylor J B and Langmuir I 1937 *Phys. Rev.* **51**(9) 753–760 URL https://link.aps.org/doi/10.1103/PhysRev.51.753

[11] 15-11-2021 Highfinesse Wavelength Meter WS/6 URL https://www.highfinesse.com/en/wavelengthmeter/wavelengthmeter-ws-6-600.html

[12] Smith P L, Heise C, Esmond J R and Kurucz R L 15-11-2021 Atomic spectral line database from CD-ROM 23 of R. L. Kurucz. URL https://lweb.cfa.harvard.edu/amp/ampdata/kurucz23/sekur.html

[13] Warner B 1968 *Monthly Notices of the Royal Astronomical Society* **139** 115–128 ISSN 0035-8711 URL https://doi.org/10.1093/mnras/139.1.115

[14] Grice R and Herschbach D 1974 *Molecular Physics* **27** 159–175 URL https://doi.org/10.1080/00268977400100131

[15] Buslov E Y and Zon B A 2012 *Phys. Rev. A* **85**(4) 042709 URL https://link.aps.org/doi/10.1103/PhysRevA.85.042709

[16] Narits A A, Mironchuk E S and Lebedev V S 2013 *Journal of Physics B: Atomic, Molecular and Optical Physics* **47** 015202 URL https://doi.org/10.1088/0953-4075/47/1/015202

[17] Desfrançois C 1995 *Phys. Rev. A* **51**(5) 3667–3675 URL https://link.aps.org/doi/10.1103/PhysRevA.51.3667

[18] Laitinen M, Rossi M, Julin J and Sajavaara T 2014 *Nuclear Instruments and Methods in Physics Research Section B: Beam Interactions with Materials and Atoms* **337** 55–61 ISSN 0168-583X URL https://www.sciencedirect.com/science/article/pii/S0168583X14006284

[19] Laulainen J, Aleiferis S, Kalvas T, Koivisto H, Kronholm R and Tarvainen O 2017 *Physics of Plasmas* **24** 103502 URL https://doi.org/10.1063/1.4998005

[20] Nørskov J K and Lundqvist B I 1979 *Phys. Rev. B* **19**(11) 5661–5665 URL https://link.aps.org/doi/10.1103/PhysRevB.19.5661

Supplementary material for manuscript "Photo-enhanced O^-, H^- and Br^- ion production in cesium sputter negative ion source - no evidence for resonant ion pair production"

A. Hossain[1], O. Tarvainen[2], M. Reponen[1], R. Kronholm[1], J. Julin[1], T. Kalvas[1], V. Toivanen[1], M. Kivekäs[1] and M. Laitinen[1]

[1]Accelerator Laboratory, Department of Physics, University of Jyväskylä, FI-40014 Jyväskylä, Finland
[2]STFC ISIS Pulsed Spallation Neutron and Muon Facility, Rutherford Appleton Laboratory, Harwell, OX11 0QX, UK

E-mail: akbar.a.hossain@jyu.fi

August 2022

1. Emission wavelength of the LE-445-6000 diode laser

The peak wavelength of the LE-445-6000 laser depends on the output power as it affects the temperature and the band gap of the diode. The emission (peak) wavelength in cw mode was recorded with Ocean Optics USB 2000+ spectrometer (1.4 nm resolution). The emission wavelengths at different output powers are shown in Table 1.

Table 1. The peak emission wavelength of the LE-445-6000 diode laser at different output powers.

Output power [W]	Emission wavelength [nm]
0.3	440.0
1.0	440.7
1.7	441.0
2.3	441.7
3.0	442.1
3.6	442.8
4.2	443.5
4.7	443.9
5.0	444.2
5.2	444.6

2. The laser power measured at the SNICS cathode

The laser power incident on the cathode surface was measured by replacing the cathode with a 1 mm diameter collimator and quartz window. The laser power passing through the collimator was measured with a power sensor (Thorlabs S142C integrating sphere photodiode) taking into account 8% absorption of the quartz window, and compared to the output power of the laser measured in front of the bending magnet viewport. The laser power delivered to the cathode was between 30%-36% of the output power for the adjustable wavelength laser (Toptica DLC DL pro HP) and 1.2%-3.0% for the LE-445-6000 diode laser after optimising the optics for the adjustable wavelength laser. The efficiency of the diode laser decreases with the output power, i.e. only 1.2% of the peak power reaches the cathode. The laser power measured from the cathode and the corresponding efficiency as a function of the output power of each laser are tabulated in Table 2.

3. Pulsing the laser with mechanical chopper vs. pulsing with the control voltage

Figure 1 demonstrates that an O^- beam current enhancement of approximately 17%, i.e. from 52.5 nA to 61.5 nA (Fig. 1(a)) and 54 nA to 63 nA (Fig. 1(b)), is observed with approximately 2.3 W (LE-445-6000 laser) laser output power with 40 Hz pulse frequency and 50% duty factor. The same result was achieved by pulsing the laser with the chopper (Fig. 1(a)) and with the control voltage (Fig. 1(b)). The rising and falling edges of the laser-induced beam current modulations are notably affected by the pulsing method as the rotating chopper blocks the laser beam only partially during a certain phase of its rotation.

4. Bromine beam current enhancement at high laser pulse repetition rate

Figure 2 shows the effect on the Br^- beam current for the LE-445-6000 diode laser with 5.2 W laser output power (444.6 nm wavelength) at different laser pulse repetition rates in the kHz-range. The prompt increase of the beam current is clearly visible in all cases when laser pulse (gray background) is applied. The given examples are measured with (a) 1 kHz, (b) 5 kHz and (c) 10 kHz laser pulse with 60% duty factor at 444.6 nm laser wavelength. The beam current enhancement is approximately (a) 28%, i.e. from 1950 nA to 2500 nA, (b) 27%, i.e. from 1850 nA to 2350 nA and (c) 24%, i.e. from 1830 nA to 2270 nA. This example provides evidence that the prompt effect on the negative beam current is clearly visible with high pulse repetition rates, up to 10 kHz.

Acknowledgements

Patent application (number 20225597) has been filed to the Finnish Patent and Registration Office.

Table 2. The output power of the two lasers, the power at the cathode and corresponding efficiency.

	Toptica DLC DL pro HP			LE-445-6000 diode laser	
Output power [mW]	Power at the cathode [mW]	Efficiency [%]	Output power [W]	Power at the cathode [mW]	Efficiency [%]
0.03	0.01	33.3	0.3	8.8	2.9
0.06	0.02	33.3	0.7	21.1	3.0
4.8	1.6	33.3	1.0	30.3	3.0
12.0	3.6	30.0	1.3	38.8	3.0
19.5	6.3	32.3	1.7	50.3	3.0
26.7	8.2	30.7	2.2	62.2	2.8
34.5	11.4	33.0	2.3	64.4	2.8
41.7	14.8	35.5	3.0	79.0	2.6
49.0	16.0	32.7	3.6	77.2	2.1
56.0	17.4	31.1	4.2	71.3	1.7
62.6	21.6	34.5	4.7	70.7	1.5
70.9	23.2	32.7	5.0	68.5	1.4
79.7	28.0	35.1	5.2	64.2	1.2
85.4	28.8	33.7	-	-	-
94.1	33.2	35.3	-	-	-
100.1	33.7	33.7	-	-	-
111.9	39.7	35.5	-	-	-
116.9	41.3	35.3	-	-	-

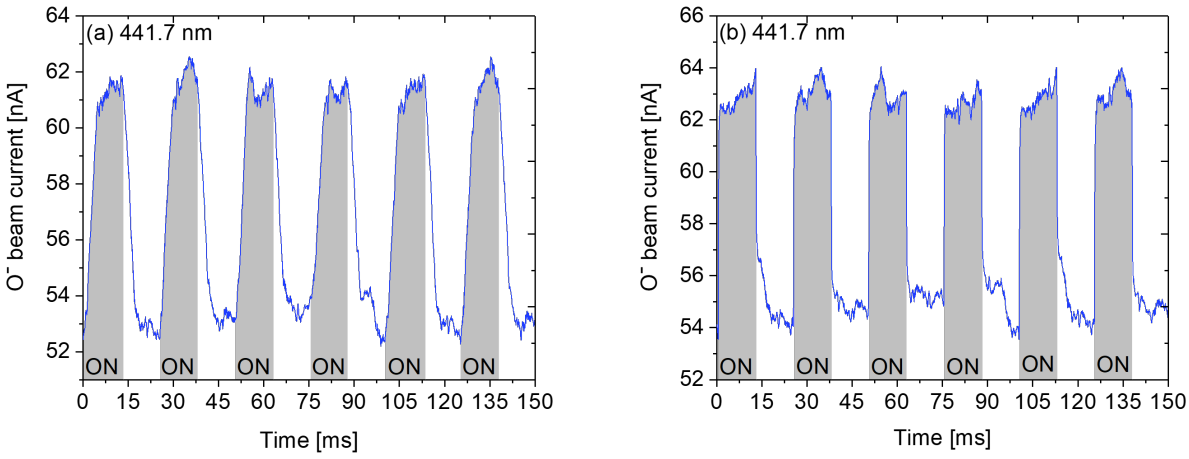

Figure 1. The effect of the LE-445-6000 diode laser on the O^- beam current. The plots show the effect with a (a) 40 Hz rotating chopper and (b) voltage controlled 40 Hz laser pulse. The duty factor is 50% in both cases.

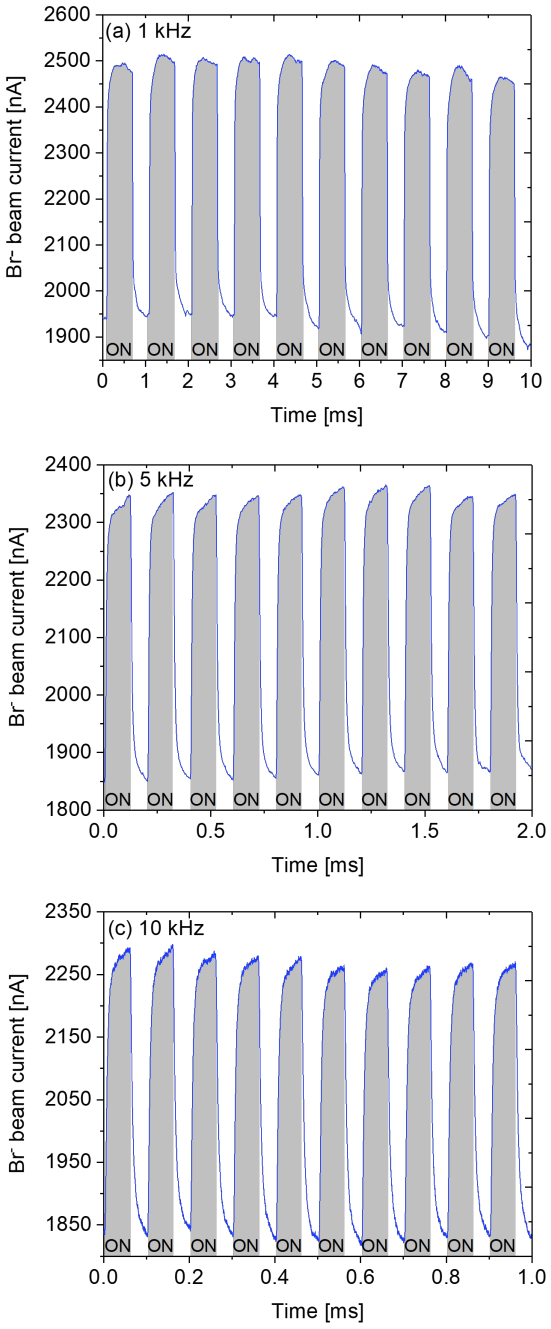

Figure 2. The effect of the LE-445-6000 diode laser on the Br^- beam current with 5.2 W laser output power (444.6 nm wavelength) at (a) 1 kHz, (b) 5 kHz and (c) 10 kHz laser pulse repetition rates. The duty factor is 60%.